Mapping of the Acetylcholine Binding Site of the Nicotinic Acetylcholine Receptor: [^{3}H]Nicotine as an Agonist Photoaffinity Label†

Richard E. Middleton and Jonathan B. Cohen*
Department of Anatomy and Neurobiology, Washington University School of Medicine, St. Louis, Missouri 63110
Received January 28, 1991; Revised Manuscript Received April 3, 1991

ABSTRACT: The agonist [^{3}H]nicotine was used as a photoaffinity label for the acetylcholine binding sites on the *Torpedo* nicotinic acetylcholine receptor (AChR). [^{3}H]Nicotine binds at equilibrium with K_{eq} = 0.6 μM to the agonist binding sites. Irradiation with 254-nm light of AChR-rich membranes equilibrated with [^{3}H]nicotine resulted in covalent incorporation into the α- and γ-subunits, which was inhibited by agonists and competitive antagonists but not by noncompetitive antagonists. Inhibition of labeling by *d*-tubocurarine demonstrated that the α-subunit was labeled via both agonist sites but the γ-subunit was labeled only via the site that binds *d*-tubocurarine with high affinity. Within the α-subunit, 93% of the labeling was contained within a 20-kDa *Staphylococcus aureus* V8 proteolytic fragment beginning at Ser-173. Sequence analysis of this peptide indicated that ≈80% of the incorporation was into Tyr-198, ≈13% was into Cys-192, and ≈7% was into Tyr-190. Chymotryptic digestion of the α-subunit confirmed that Tyr-198 was the principal amino acid labeled by [^{3}H]nicotine. This confirmation required a novel radiosequencing strategy employing *o*-phthalaldehyde, since the efficiency of photolabeling was low (≈1.0%) and the labeled chymotryptic peptide was not isolated in sufficient quantity to be identified by mass. [^{3}H]Nicotine, which is the first photoaffinity agonist used, labels primarily Tyr-198 in contrast to competitive antagonist affinity labels, which label primarily Tyr-190 and Cys-192/Cys-193.

Ligand-gated ion channels generate rapid changes of membrane potential upon binding neurotransmitter. The recent isolation and cloning of cDNAs encoding the subunits of several ligand-gated ion channels has revealed that these proteins are homologous members of a protein superfamily (Betz, 1990). The most thoroughly characterized member of this superfamily is the nicotinic acetylcholine receptor (AChR)[1] of *Torpedo* electric organ (Popot & Changeux, 1984; Claudio, 1989, Stroud et al., 1990). The *Torpedo* AChR is composed of four homologous subunits in a stoichiometry of $\alpha_2\beta\gamma\delta$ (Raftery et al., 1980; Noda et al., 1983). All subunits span the lipid bilayer and are arranged pseudosymmetrically about a central axis assumed to correspond to the ion channel (Kubalek et al., 1987; Toyoshima & Unwin, 1988; Mitra et al., 1989).

The AChR has two binding sites for agonists and competitive antagonists. On the basis of analysis of equilibrium binding, the two sites bind agonists equivalently (or with positive cooperativity), while competitive antagonists such as *d*-tubocurarine bind to the sites with widely different affinities (Neubig & Cohen, 1979; Weiland & Taylor, 1979). The AChR also contains one high-affinity binding site for amine noncompetitive antagonists that is coupled allosterically to the agonist sites. The binding of most noncompetitive antagonists enhances agonist equilibrium binding affinity and vice versa (Krodel et al., 1979; Heidmann et al., 1983; Cohen et al., 1985). Photoaffinity labeling studies indicate that homologous regions from each AChR subunit contribute to the structure of the noncompetitive antagonist binding site (Hucho et al., 1986; Giraudat et al., 1987; Revah et al., 1990).

Several competitive antagonist affinity labels have been used to identify specific amino acids contributing to the agonist binding site. The residues labeled lie primarily within the α-subunit, in the vicinity of Cys-192 and Cys-193, which form a vicinal disulfide (Kao & Karlin, 1986; Kellaris & Ware, 1989) that is conserved in α-subunits of all muscle and neuronal nicotinic AChR's. [^{3}H]-4-(*N*-maleimido)-α-benzyltrimethylammonium (MBTA), which alkylates the α-subunit only after disulfide reduction, reacts solely with Cys-192 and Cys-193 (Kao et al., 1984). [^{3}H]Lophotoxin analogue 1, an uncharged diterpine isolated from gorgonian corals, specifically alkylates Tyr-190 in the α-subunit (Abramson et al., 1989). In the presence of the noncompetitive antagonist phencyclidine, [^{3}H]-*p*-(dimethylamino)benzenediazonium fluoroborate binds weakly ($K \approx 1$ mM) to the acetylcholine (ACh) site but can be photoincorporated efficiently into the α-subunit, with 60% of specific labeling associated with Tyr-190, Cys-192, and Cys-193 and lesser amounts with Trp-149 (5%) and Tyr-93 (5%) (Dennis et al., 1988; Galzi et al., 1990). In addition to contributions from the α-subunit, the pattern of photolabeling of AChR by [^{3}H]-*d*-tubocurarine indicates that the ACh binding sites are actually at the interface of AChR subunits, with one site at the α–γ interface (the site binding *d*-tubocurarine with high affinity) and the other at the α–δ interface (Pedersen & Cohen, 1990).

While agonists and competitive antagonists bind in a mutually exclusive manner, it remains to be determined whether the same amino acids are important for the recognition of agonists as well as antagonists. This is of particular interest because the binding of antagonists does not produce the same changes of AChR structure as the binding of agonists. Antagonists do not open the channel (a nonequilibrium change),

† This research was supported in part by USPHS Grants NS 19522 and NS 22828 (Senator Jacob Javits Center for Excellence in Neuroscience). R.E.M. was supported in part by a Lucille P. Markey Charitable Trust Grant No. 84-17.

[1] Abbreviations: AChR, nicotinic acetylcholine receptor; ACh, acetylcholine; GSSG, oxidized glutathione; H_{10}-HTX, *d,l*-decahydro(pentenyl)histrionicotoxin; IAA, iodoacetamide; OPA, *o*-phthalaldehyde; PAGE, polyacrylamide gel electrophoresis; SDS, sodium dodecyl sulfate; TFA, trifluoroacetic acid; TPS, *Torpedo* physiological saline (250 mM NaCl, 5 mM KCl, 3 mM $CaCl_2$, 2 mM $MgCl_2$, 5 mM sodium phosphate, pH 7.0); V8 protease, *S. aureus* V8 protease.

0006-2960/91/0430-6987$02.50/0

and antagonists bind with similar affinity to resting and desensitized states of the AChR while agonists bind with 10^5-fold greater affinity to the desensitized state than to the resting state (Neubig et al., 1982).

The only agonist affinity label that has been characterized is bromoacetylcholine, which like MBTA only alkylates α-subunit in reduced AChR, presumably on Cys-192 and Cys-193 (Damle et al., 1978). In this report we utilize [^{3}H]nicotine as an agonist photoaffinity label. Nicotine is an agonist for *Torpedo* AChR (Forman et al., 1987), and on the basis of its dose-dependent inhibition of [^{125}I]-α-bungarotoxin binding (Weiland & Taylor, 1979), nicotine binds with high affinity ($K_{eq} \approx 1$ μM) to the ACh binding sites. Nicotine itself as well as other substituted pyridines and pyrrolidines are known to undergo complex photoaddition reactions (Caplain et al., 1971; Whitten, 1976; Singh et al., 1980). We characterize the equilibrium binding of [^{3}H]nicotine and demonstrate that it can be photoincorporated into the ACh sites of the *Torpedo* AChR. Both the α- and γ-subunits are photolabeled in a pharmacologically specific manner, and within the α-subunit Tyr-198 is shown to be the primary site of photolabeling.

Experimental Procedures

Materials. AChR-rich membranes were isolated from the electric organs of *Torpedo californica* (Marinus, Inc., Westchester, CA) by the method of Sobel et al. (1977) with the modifications described previously (Pedersen et al., 1986) except that the homogenization buffer also contained 15 mg each of Calpain inhibitors I and II (Boehringer Mannheim). The final membrane pool was stored in 38% sucrose/0.02% NaN_3 at −80 °C under argon and contained 1.4–1.8 nmol of acetylcholine binding sites/mg of protein, as measured with [^{3}H]acetylcholine in an microultracentrifugation assay (Krodel et al., 1979).

[^{3}H]Nicotine (L-(−)-[*N-methyl*-^{3}H]nicotine, 67 Ci/mmol) and Enhance were purchased from New England Nuclear. [^{3}H]Nicotine was repurified by thin-layer chromatography so that radiochemical purity was always greater than 90% as determined by HPLC. [^{14}C]Iodoacetamide (57 mCi/mmol) was from Amersham. *d,l*-Decahydro(pentenyl)histrionicotoxin (H_{10}-HTX) was kindly donated by Dr. Y. Kishi (Harvard University) and proadifen by Smith, Kline, and French. α-Bungarotoxin was from Biotoxins Inc.; phencyclidine was from Alltech Associates, and *Staphylococcus aureus* V8 protease (V8 protease) was from ICN Biochemicals. Trifluoroacetic acid (TFA), *o*-phthalaldehyde (OPA), Lubrol-PX, and mercaptoethanol were from Pierce. Carbamylcholine chloride, (−)-nicotine di-(+)-tartrate salt, *d*-tubocurarine chloride, oxidized glutathione (GSSG), TLCK–chymotrypsin, iodoacetamide (IAA), and endoglycosidase H were from Sigma Chemical Co.

[^{3}H]Nicotine Binding. The equilibrium binding of [^{3}H]-nicotine (0.3–2.7 Ci/mmol) to AChR-rich membranes in *Torpedo* physiological saline (TPS) was measured at ambient temperature by a Beckman airfuge microultracentrifugation assay described in detail by Krodel et al. (1979) for the binding of [^{14}C]meproadifen. Nonspecific binding of [^{3}H]nicotine was determined in the presence of 0.4 mM carbamylcholine and was a linear function of the free [^{3}H]nicotine concentration at least up to 15 μM.

Photolabeling of AChR-Rich Membranes with [^{3}H]-Nicotine. For analytical labeling experiments, membrane suspensions (0.2–1.7 mg/mL) in a volume of 30–150 μL of TPS/1 mM GSSG were equilibrated with [^{3}H]nicotine (12.0–64.0 Ci/mmol) and cholinergic ligands and then irradiated for 10 min with a Spectroline 254-nm hand-held lamp as described by Pedersen and Cohen (1990). Polypeptides were resolved by SDS–PAGE, and the incorporation of [^{3}H]nicotine was determined by fluorography as described by Pedersen et al. (1986). Incorporation of radioactivity into individual polypeptides was quantified by scintillation counting of gel slices as described by Dreyer et al. (1986) except that 10% (v/v) TS-1 tissue solubilizer (RPI) was used and the scintillation counting efficiency was ≈25%. Nonspecific labeling was determined in the presence of 0.3 mM carbamylcholine and was a linear function of the free [^{3}H]nicotine concentration. The same conditions were used for preparative labeling (5–10 mg of membranes) with [^{3}H]nicotine (10–14 Ci/mmol) except that stirred membrane suspensions (3–6 mL) were irradiated for 4–5 min in plastic weigh boats (VWR No. 12577-005).

Data Analysis. Equilibrium binding of [^{3}H]nicotine and concentration dependence of subunit labeling were fit by the nonlinear least-squares program of RS/1 (BBN Software) to the general form $[B = A/(1 + (K_{eq}/L)) + (mL + d)]$, where B is the bound [^{3}H]nicotine (or counts per minute incorporated), A is the maximum specific binding (or counts per minute incorporated), K_{eq} is the dissociation constant (or apparent dissociation constant K_{ap}), L is the measured free [^{3}H]nicotine concentration, m is the slope of nonspecific binding (or labeling) determined in parallel experiments performed in the presence of excess carbamylcholine, and d is the independently determined background counts per minute. Inhibition of binding and of photolabeling by carbamylcholine and *d*-tubocurarine was fit to functions representing competition for binding at one $[B = A/(1 + (I/K)^n) + \text{NSP}]$ or two $[B = A/(1 + (I/K_1)) + A/(1 + (I/K_2)) + \text{NSP}]$ sites, where B is the total [^{3}H]nicotine bound (or counts per minute incorporated), A is the maximum specifically bound [^{3}H]nicotine (or counts per minute incorporated) for the fixed [^{3}H]nicotine concentration used, I is the total inhibitor concentration, K is the total inhibitor concentration that yields 50% inhibition, and NSP is the nonspecific binding (or labeling) that was not treated as an adjustable parameter. Data were fit both with $n = 1$ and with n as an adjustable parameter. Errors are reported as ± standard error.

Reaction of AChR-Rich Membranes with [^{14}C]Iodoacetamide (IAA). A method for selective reduction and alkylation of the vicinal disulfide Cys-192/Cys-193 in the α-subunit has been described (Kao & Karlin, 1986). We used this procedure to selectively and quantitatively label α-subunit with [^{14}C]IAA at Cys-192 and Cys-193 for use in experiments assessing the effectiveness of digestion conditions for this region of the α-subunit. AChR-rich membranes (7.2 mg) were prealkylated with 3 mM nonradioactive IAA for 1 h and then washed with reducing buffer (150 mM NaCl, 1.5 mM EDTA, 15 mM Tris, pH 8.0, and 4.5 mM NaN_3) and resuspended in 1 mL of 0.3 mM dithiothreitol in reducing buffer. After 1 h, the suspension was reacted for 60 min with 2.5 mM [^{14}C]IAA (1 Ci/mol). The membranes were then collected by ultracentrifugation, and the α-subunit was purified as described below. The incorporation was 2.7 mol of ^{14}C/mol of α-subunit as measured by amido black protein assay (Schaffner & Weissman, 1973). For membranes previously photolabeled with [^{3}H]nicotine, the same procedure was used except that the membranes were prealkylated in 1 mL of 1 mM IAA, reduced in 0.5 mL of 0.3 mM dithiothreitol, and alkylated with the addition of 0.5 mL of 2 mM [^{14}C]IAA (21 Ci/mol). In two such isolations of [^{3}H]nicotine-labeled α-subunit, 2.1 and 1.9 mol of ^{14}C were incorporated/mole of α-subunit, and in one experiment using α-subunit photolabeled in the presence of carbamylcholine,

α-subunit contained 1.9 mol of ^{14}C/mol of α-subunit. For [^{3}H]nicotine-labeled membranes that were alkylated with nonradioactive IAA, the membranes after photolabeling were resuspended directly in 0.3 mM dithiothreitol without prealkylation with IAA.

Purification of [^{3}H]Nicotine-Labeled α-Subunit. AChR α-subunit was isolated by electrophoresis on preparative slab gels (14 × 16 cm, 1.5 mm thick). After being photolabeled with [^{3}H]nicotine, AChR-rich membranes (5–8 mg) were dissolved in Laemmli sample buffer and the polypeptides were resolved on an 8% slab gel as described by Pedersen et al. (1986). The α-subunit was excised from the gel and eluted by soaking gel fragments overnight in 10 mL of elution buffer (0.25% SDS/100 mM NH_4HCO_3, pH 8.4/1.0 mM DTT). Gel fragments were removed by filtration, and the filtrate was concentrated to ≈0.5 mL in a Centriprep 30 concentrator (Amicon). Protein was precipitated with 5 volumes of acetone (1 h at −20 °C) and resuspended in 10 mM sodium phosphate, pH 7.0/0.1% SDS/1.0 mM EDTA/1.0 mM DTT. As determined by protein assay, the recovery of α-subunit varied between 50 and 80%.

Enzymatic Digestions and Peptide Purification. Proteolytic mapping of the α-subunit with *S. aureus* V8 protease was performed according to the procedure of Cleveland et al. (1977) as described by White and Cohen (1988). Analytical experiments on [^{3}H]nicotine-labeled α-subunit (25–30 μg) were analyzed by fluorography and by scintillation counting of gel slices. Preparative experiments were also performed as described by White and Cohen (1988) except that [^{3}H]-nicotine-labeled membranes (10 mg) were first digested overnight with 50 milliunits of endoglycosidase H in 1.5 mL of digestion buffer (50 mM sodium phosphate, pH 7.0/1.0% SDS). Peptides were recovered by the passive elution procedure described above using a Centriprep 10 concentrator.

Purified [^{3}H]nicotine- and/or [^{14}C]IAA-labeled α-subunit (10–100 μg) was digested for 12 h at ambient temperature with 20% (w/w) TLCK–chymotrypsin in resuspension buffer/0.1 M NH_4HCO_3, pH 8.1/0.5% Lubrol-PX. The digests were adjusted to 1.0% trifluoroacetic acid (TFA) and fractionated on a reversed-phase HPLC system consisting of a Waters Model 680 gradient controller and two Model 510 pumps, a Vydac C_{18} (218TP54) column, and a Kratos Spectroflow 757 absorbance detector. Samples were eluted with gradients of water/0.1% TFA (solvent A) vs acetonitrile/0.09%TFA (solvent B) at 0.5 mL/min. Fractions of 0.5 mL were collected, and the radioactivity was monitored by scintillation counting. Fractions containing peptides of interest were pooled and either vacuum centrifuged to dryness or stored frozen at −80 °C.

Peptide Sequencing. Sequential Edman degradation of peptides was performed as described by Carr et al. (1987). To test for the presence of ^{3}H-labeled peptides below the level of mass detection, *o*-phthalaldehyde (OPA) was used to react with all primary amines at cycles predicted to expose an amino-terminal proline residue (Brauer et al., 1984). When samples were reacted with OPA during a sequencing run, the sequencer was paused after the cycle that exposed the appropriate amino acid. The filter was treated for 20 s with 12.5% aqueous trimethylamine and dried with argon for 2 min. The filter cartridge was disassembled and 30 μL of OPA reagent (2.0 mg of OPA/mL in acetonitrile/0.5% mercaptoethanol) was added to the sample filter. The cartridge was immediately reassembled and treated with 12.5% aqueous trimethylamine for 10 min. The filter was dried with argon for 2 min, washed with ethyl acetate for 5 min, and dried for another 2 min with argon. Normal sequencing was then resumed.

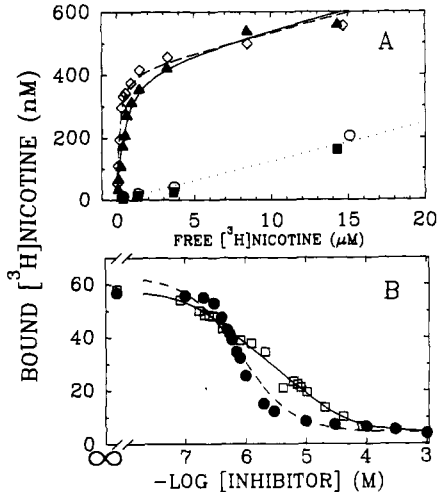

FIGURE 1: Equilibrium binding of [^{3}H]nicotine to AChR-rich membranes. AChR-rich membranes (45 μg) were suspended in 100 μL of TPS (0.6 μM ACh sites) and equilibrated with [^{3}H]nicotine and other cholinergic ligands for 30 min. Membranes were centrifuged to measure the free and bound [^{3}H]nicotine concentrations as described under Experimental Procedures. (A) Samples were incubated with various [^{3}H]nicotine concentrations in the absence (◇, ▲) or presence (○, ■) of 0.4 mM carbamylcholine to define nonspecific binding and with (◇, ○) or without (▲, ■) 30 μM proadifen. Symbols represent the average of duplicate determinations and lines are nonlinear least-squares fits to the data as described under Experimental Procedures. The K_{eq} was 0.49 ± 0.04 and 0.14 ± 0.02 μM in the absence and presence of proadifen, respectively, and the total sites were 0.43 ± 0.01 and 0.42 ± 0.01 μM. (B) Samples were incubated with 100 nM [^{3}H]nicotine/30 μM proadifen with various concentrations of carbamylcholine (●) and *d*-tubocurarine (□). Data were fit to one-site (●) or two-site (□) inhibition functions (n = 1) as described under Experimental Procedures. For carbamylcholine, K = 0.8 ± 0.08 μM and for *d*-tubocurarine K_1 = 0.5 ± 0.08 μM and K_2 = 10.2 ± 0.9 μM.

RESULTS

[^{3}H]Nicotine Equilibrium Binding. Equilibrium binding of [^{3}H]nicotine to AChR-rich membranes was quantified to establish whether binding was specific for the agonist site and to determine equilibrium binding constants. Binding was measured by ultracentrifugation in the presence of free [^{3}H]nicotine concentrations varying from 0.4 to 15 μM in the absence or presence of the agonist carbamylcholine (0.4 mM) or the noncompetitive antagonist proadifen (30 μM) (Figure 1A). Binding in the presence of carbamylcholine increased linearly with concentration, and that binding was the same in the absence (m = 0.011 ± 0.004, n = 7) or presence (m = 0.012 ± 0.003, n = 4) of proadifen. In the absence of proadifen the specific component of binding was accounted for by a simple hyperbolic binding function (K_{eq} = 0.6 ± 0.1 μM, n = 7). In the presence of proadifen the specific binding was again hyperbolic and [^{3}H]nicotine bound to the same number of sites but with 3-fold higher affinity (K_{eq} = 0.22 ± 0.05 μM, n = 4). The inhibition of [^{3}H]nicotine binding by carbamylcholine and its allosteric regulation by proadifen indicated that [^{3}H]nicotine was binding to the ACh binding sites on the AChR and not to the noncompetitive antagonist site.

The AChR has two binding sites for agonists, both that bind carbamylcholine at equilibrium with equal affinity (K_{eq} = 0.1 μM; Boyd & Cohen, 1980), but one agonist site binds the antagonist *d*-tubocurarine with high affinity (K_1 = 30 nM) and the other with low affinity (K_2 = 7 μM; Neubig & Cohen, 1979; Pedersen & Cohen, 1990). When [^{3}H]nicotine binding

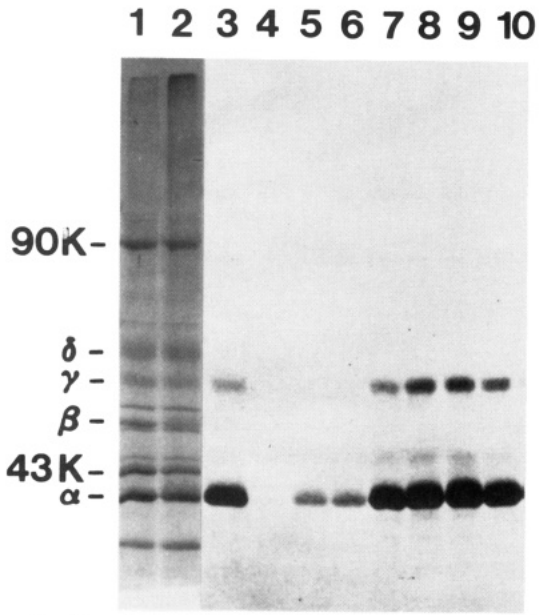

FIGURE 2: Photoincorporation of [^{3}H]nicotine into AChR-rich membranes. AChR-rich membranes (34 μg) were suspended in 30 μL of TPS (2 μM ACh sites) with 1 μM [^{3}H]nicotine/1 mM GSSG and irradiated for 10 min at 254 nm. Polypeptides were separated by SDS–PAGE, visualized by Coomassie blue stain (lanes 1 and 2), and processed for fluorography (lanes 3–10). Coomassie stains of samples prior to (lane 1) and after (lane 2) 10-min irradiation are shown. Membrane suspensions contained no other cholinergic ligands (lanes 2, 3, and 7), 0.3 mM carbamylcholine (lane 4), 10 μM *d*-tubocurarine (lane 5), 10 μM α-bungarotoxin (lane 6), 30 μM H_{10}-HTX (lane 8), 30 μM proadifen (lane 9), or 30 μM phencyclidine (lane 10).

was measured in parallel with [^{3}H]ACh binding, the number of [^{3}H]nicotine sites was similar to but less than (80%, n = 2) the number of ACh sites. Errors in the determination of the radiochemical purity and/or specific activity of either ligand could account for the discrepancy in the number of sites, and the observed concentration dependence of the inhibition of [^{3}H]nicotine binding by *d*-tubocurarine indicated that [^{3}H]nicotine did bind to both ACh sites (Figure 1B). High concentrations of *d*-tubocurarine inhibited [^{3}H]nicotine binding to the same extent as carbamylcholine, and the concentration dependence was fit by a two-site model with K_1 = 0.5 μM and K_2 = 10 μM (or by a single-site model with K = 2.2 μM, n = 0.68 ± 0.03). Inhibition by carbamylcholine was characterized by a K = 0.8 μM, consistent with its equilibrium binding, and this inhibition was best fit with a Hill coefficient, n = 1.7 ± 0.1. While $n > 1$ might result in part from cooperative binding, it is also expected for the assay conditions used where the concentration of binding sites (0.6 μM) exceeded the inhibitor dissociation constant.

Photoincorporation of [^{3}H]Nicotine into AChR-Rich Membranes. In initial experiments, membranes equilibrated with [^{3}H]nicotine were irradiated at 254 nm for various times and analyzed by SDS–PAGE. After 10 min of irradiation there was evidence of photochemical cross-linking as judged by the decrease of AChR subunit mass (Coomassie stain) and an associated increase in high molecular weight material in the gel (Figure 2, lane 1 vs 2). Photochemical cross-linking became more serious at longer irradiation times (data not shown), and thus sample irradiation was limited to 10 min. The pattern of [^{3}H]nicotine incorporation was analyzed by SDS–PAGE with subsequent fluorography as well as by scintillation counting of excised gel fragments. While the principal component of [^{3}H]nicotine incorporation was into the AChR α-subunit, the γ-subunit also clearly incorporated

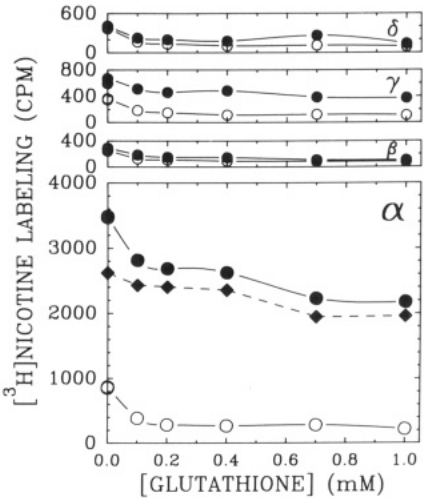

FIGURE 3: Oxidized glutathione reduces nonspecific photoincorporation of [^{3}H]nicotine into the AChR subunits. AChR-rich membranes (34 μg) were suspended in 30 μL of TPS (2 μM ACh sites)/5 μM [^{3}H]nicotine/30 μM proadifen with various concentrations of GSSG in the absence (●) or presence (○) of 0.3 mM carbamylcholine. After irradiation for 10 min at 254 nm, the samples were solubilized, and the polypeptides were resolved by SDS–PAGE and visualized by Coomassie blue stain. The counts per minute of [^{3}H]nicotine incorporated into each AChR subunit (α, β, γ, δ) was determined as described under Experimental Procedures and is plotted versus the GSSG concentration. Specific labeling (◆) is the difference between the total labeling (●) and the nonspecific labeling (○).

label (Figure 2, lanes 3 and 7). The labeling of both the α- and γ-subunits was inhibited by carbamylcholine, *d*-tubocurarine, and α-bungarotoxin (Figure 2, lanes 4–6) but not by the noncompetitive antagonists H_{10}-HTX, proadifen, or phencyclidine (lanes 8–10). In fact, noncompetitive antagonists increased incorporation into the α- and γ-subunits, presumably by decreasing the K_{eq} for [^{3}H]nicotine. A minor specifically labeled component with slightly lower mobility than the 43K protein has previously been shown to be the α-subunit whose mobility has been altered by UV irradiation (Pedersen & Cohen, 1990).

To determine whether photolabeling occurred after [^{3}H]-nicotine diffused away from its binding site, methionine and oxidized glutathione (GSSG) were examined as potential photochemical scavengers. Methionine (10 mM) had little effect on the pattern of photoincorporation, but GSSG substantially reduced nonspecific labeling with little effect on specific incorporation of [^{3}H]nicotine into the α- and γ-subunits (Figure 3). GSSG (1 mM) reduced the nonspecific incorporation of [^{3}H]nicotine into the α- and γ-subunits by ≈75% and the specific incorporation by 25 and 13%, respectively. The reduction in specific labeling is consistent with the expected absorption of 254-nm light by 1 mM GSSG, which under the conditions of labeling is ≈15%. In the presence of 1 mM GSSG, 0.46 and 0.12% of α- and γ-subunits were labeled specifically. The level of carbamylcholine-sensitive incorporation into the β- and δ-subunits was less than 2% of the labeling of α-subunit.

Specificity of [^{3}H]Nicotine Photoincorporation into the α- and γ-Subunits. The concentration dependence of [^{3}H]-nicotine photoincorporation into both the α- and γ-subunits was measured in the absence and presence of proadifen (Figure 4). The nonspecific incorporation was measured in the presence of 0.3 mM carbamylcholine and was essentially the same in the absence and presence of proadifen. The K_{ap}'s for labeling of the α- and γ-subunits were the same and equal to 1.5 μM in the absence of proadifen and 0.6 μM in its presence. These values are similar to those determined in equilibrium

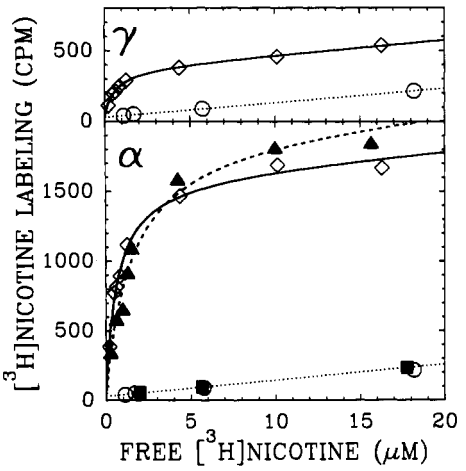

FIGURE 4: Concentration dependence of [^{3}H]nicotine labeling of α- and γ-subunits. AChR-rich membranes (34 μg) were suspended in 30 μL of TPS/1 mM GSSG (2 μM ACh sites) with various concentrations of [^{3}H]nicotine, in the absence (◇, ▲) or presence (○, ■) of 0.3 mM carbamylcholine and with (◇, ○) or without (▲, ■) 30 μM proadifen. Membrane suspensions were irradiated, and the [^{3}H]nicotine incorporation into α- and γ-subunits was determined as described in Figure 3. Lines represent nonlinear least-squares fits to the data as described under Experimental Procedures. The K_{ap}'s for labeling of the α- and γ-subunits in the absence of proadifen were 1.5 ± 0.2 and 1.6 ± 0.2 μM (data not shown), respectively, and in the presence of proadifen were 0.65 ± 0.05 and 0.60 ± 0.04 μM, respectively. The maximum counts per minute incorporated in the absence of proadifen represented labeling of 0.43% (1900 cpm) and 0.20% (440 cpm) of the α- and γ-subunits, respectively, and in the presence of proadifen represented labeling of 0.36% (1600 cpm) and 0.16% (350 cpm) of subunits.

binding experiments, with the slightly higher K_{ap} values here probably due to uncertainties in the estimated free [^{3}H]nicotine concentration as a result of [^{3}H]nicotine photodegradation.

The inhibition of labeling by carbamylcholine and *d*-tubocurarine was studied to determine whether the [^{3}H]nicotine photoincorporation into the α- and γ-subunits resulted from [^{3}H]nicotine binding to one or both agonist sites. The inhibition of labeling with *d*-tubocurarine was dramatically different for the α- and γ-subunits (Figure 5). With use of a single-site fit with a variable Hill coefficient, the IC_{50} for the γ-subunit (160 ± 8 nM) was close to that for the α-subunit (375 ± 80 nM), but the Hill coefficient (n) for inhibition of α-subunit labeling was 0.7 ± 0.09 whereas for the γ-subunit it was 1.9 ± 0.1. Carbamylcholine inhibited the α- and γ-subunit incorporation with IC_{50}'s of 430 ± 40 and 477 ± 47 nM and with Hill coefficients of 1.6 ± 0.2 and 1.6 ± 0.2, respectively (Figure 5). Inhibition of [^{3}H]nicotine incorporation into the α-subunit by *d*-tubocurarine was fit with a Hill coefficient similar to that used for the inhibition of [^{3}H]nicotine binding and is consistent with labeling of α-subunit via both agonist binding sites.[2] The [^{3}H]nicotine incorporation into

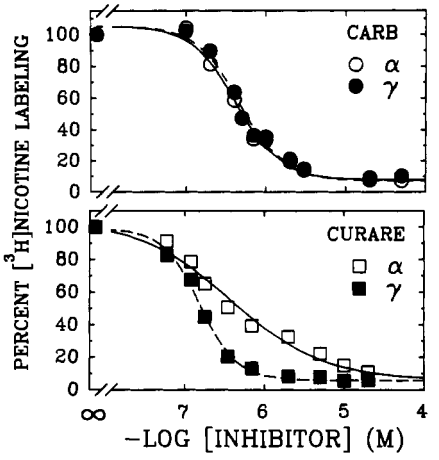

FIGURE 5: Inhibition of [^{3}H]nicotine photoincorporation into the α- and γ-subunits by carbamylcholine and *d*-tubocurarine. AChR-rich membranes (34 μg) were suspended in 150 μL of TPS (0.4 μM ACh sites) with 0.3 μM [^{3}H]nicotine/1 mM GSSG/20 μM proadifen and various concentrations of inhibitor. The membrane suspensions were irradiated and the [^{3}H]nicotine incorporation was determined as described in Figure 3. [^{3}H]Nicotine labeling (as percent of labeling in the absence of inhibitor) of the α- (○, □) and γ-subunits (●, ■) is plotted versus the total concentration of carbamylcholine (top) or *d*-tubocurarine (bottom, average of two experiments). Data were fit with a one-site inhibition function allowing a free fit to a Hill coefficient (n) as described under Experimental Procedures. For carbamylcholine K = 0.43 ± 0.04 and 0.48 ± 0.05 μM for the α- and γ-subunits, respectively, and for *d*-tubocurarine K = 0.38 ± 0.09 and 0.16 ± 0.008 μM for the α- and γ-subunits, respectively. The Hill coefficients (n) for inhibition of [^{3}H]nicotine labeling by carbamylcholine were 1.6 ± 0.2 for both the α- and γ-subunits but for the inhibition by *d*-tubocurarine were 0.74 ± 0.09 and 1.86 ± 0.15 for the α- and γ-subunits, respectively. The inhibition of [^{3}H]nicotine labeling of the α-subunit by *d*-tubocurarine (□) was also fit to a two-site inhibition function (constrained to two equal sites) with K_1 = 0.12 ± 0.05 and K_2 = 1.4 ± 0.44 μM. For the experiment with carbamylcholine, total incorporation into α- and γ-subunits was 1070 and 360 cpm, respectively, and for the *d*-tubocurarine experiment, total incorporation into α- and γ-subunits was 1410 and 440 cpm.

the γ-subunit was completely inhibited by low concentrations of *d*-tubocurarine and with $n > 1$, as would be expected if the γ-subunit was labeled only by [^{3}H]nicotine bound to the site with high affinity for *d*-tubocurarine.

Mapping of the [^{3}H]Nicotine-Labeled Sites in α-Subunit with V8 Protease. To localize the sites of labeling within the α-subunit, [^{3}H]nicotine-labeled α-subunit was digested with V8 protease under conditions that generate four fragments readily resolvable by SDS–PAGE (Figure 6A). The two largest fragments, containing ≈ two-thirds of the total α-subunit mass, are a 20-kDa peptide (V8-20) beginning at Ser-173 and an 18-kDa peptide (V8-18) beginning at Val-46 (Pedersen et al., 1986). If the α-subunit is treated with endoglycosidase H prior to digestion (Figure 6, lanes 3 and 4), V8-18, which contains the single N-linked carbohydrate in the α-subunit, is converted to a 12-kDa peptide (V8-12). The amino termini of the 10-kDa (V8-10) and 4kDa (V8-4) fragments have been identified as Asn-339 and Ser-1, respectively (White & Cohen, 1988). On the basis of fluorography (Figure 6B), [^{3}H]nicotine was incorporated only into V8-20. On the basis of liquid scintillation counting of the four V8 proteolytic fragments after gel excision, V8-20 contained 93% of the specific label in the α-subunit. Approximately 3% of the specific label was found in each of the V8-18 and V8-10 fragments. Ninety-five percent of the incorporation into V8-20 was inhibited by carbamylcholine.

Identification of the Amino Acids Labeled by [^{3}H]Nicotine by Sequence Analysis of V8-20. Preparative slab gel electrophoresis was used to isolate V8-20 from [^{3}H]nicotine-labeled

[2] The *d*-tubocurarine inhibition of reversible binding and of α-subunit photolabeling are both fit by n = 0.7 ± 0.1, consistent with α-subunit labeling via both agonist sites. When data are fit in terms of a two-site model with equal occupancy (or photolabeling) by [^{3}H]nicotine, the parameters for *d*-tubocurarine inhibition of binding (Figure 1B: K_1 = 0.5 ± 0.1 μM, K_2 = 10 ± 1 μM) differ from those for inhibition of α-subunit photolabeling (Figure 5: K_1 = 0.12 ± 0.05 μM, K_2 = 1.4 ± 0.4 μM). This difference has been seen in several independent experiments. We believe this difference results from constraining the fits to equal contributions from the two sites while in fact there is preferential photoincorporation into the site with high affinity for *d*-tubocurarine. Additional experimentation will be required to generate sufficient data to allow analysis of the inhibition curves in terms of models including three rather than two adjustable parameters.

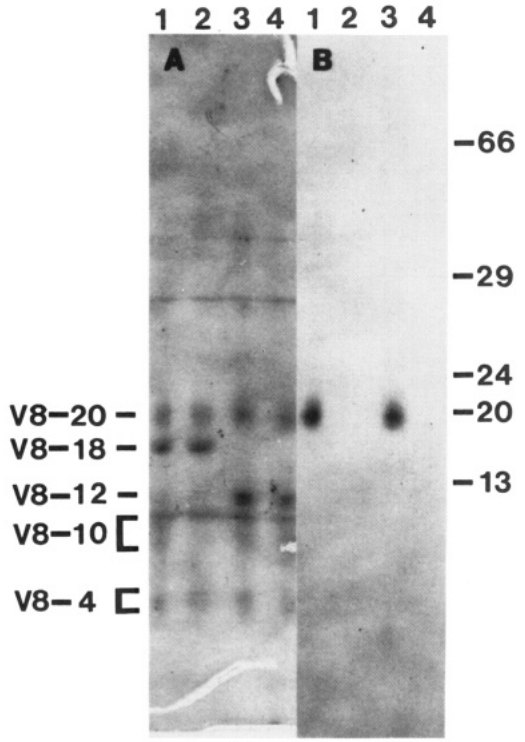

FIGURE 6: Proteolytic mapping of [^{3}H]nicotine incorporation into the α-subunit using *S. aureus* V8 protease. AChR-rich membranes (500 μg) were suspended in 450 μL of TPS (2 μM ACh sites) with 4 μM [^{3}H]nicotine/1 mM GSSG/20 μM proadifen in the absence (lanes 1 and 3) or presence (lanes 2 and 4) of 0.3 mM carbamylcholine. Membrane suspensions were irradiated for 10 min at 254 nm and then pelleted, and the membrane pellets were resuspended in 50 mM sodium phosphate, pH 7.0/1.0% SDS (47 μL) for digestion in the absence (lanes 1 and 2) or presence (lanes 3 and 4) of 4.3 milliunits of endoglycosidase H. [^{3}H]Nicotine-labeled α-subunit was resolved by SDS–PAGE and then excised for digestion with 3 μg of V8 protease in a proteolytic mapping gel as described under Experimental Procedures. The mapping gel was stained with Coomassie blue (panel A) and subjected to fluorography for 4 weeks (panel B). The V8 fragments are labeled by the nomenclature of White and Cohen (1988), and the molecular weight standards are bovine albumin (66 000), carbonic anhydrase (29 000), trypsinogen (24 000), trypsin inhibitor (20 000), and cytochrome *c* (13 000).

AChR α-subunit. To minimize possible contamination of V8-20 by V8-18 (Pedersen et al., 1986), labeled AChR was digested with endoglycosidase H prior to α-subunit isolation. From 10 mg of AChR-rich membranes (18 nmol of α-subunit) labeled in the presence of 5 μM [^{3}H]nicotine, 6 nmol of V8-20 was recovered containing 1200 cpm/μg ($\approx$0.3% of α-subunit labeled). Ninety-four percent of the labeling of V8-20 was specific, since V8-20 isolated from AChR labeled in the presence of carbamylcholine contained only 70 cpm/μg. Fragment V8-12, which was also recovered at $\approx$30% yield, contained only 25 cpm/μg.

Labeled α-subunit (40 μg, 50 000 cpm) and V8-20 (40 μg, 45 000 cpm) were subjected to 38 cycles of automated sequential Edman degradation with portions of each cycle analyzed for release of PTH-amino acids and tritium. As expected, the sequence of the intact α-subunit began at Ser-1. The repetitive yield of sequencing was 93% (data not shown), and in each cycle there was a background release of tritium of $\approx$0.5% of the total amount loaded with no significant release detected above that level (Figure 7B). When V8-20 was sequenced, the background level of release in each cycle was similar to that of intact α-subunit, but there was significant release of tritium above that level in cycles 18 and 20 with the largest level of release in cycle 26 (Figure 7A). The tritium

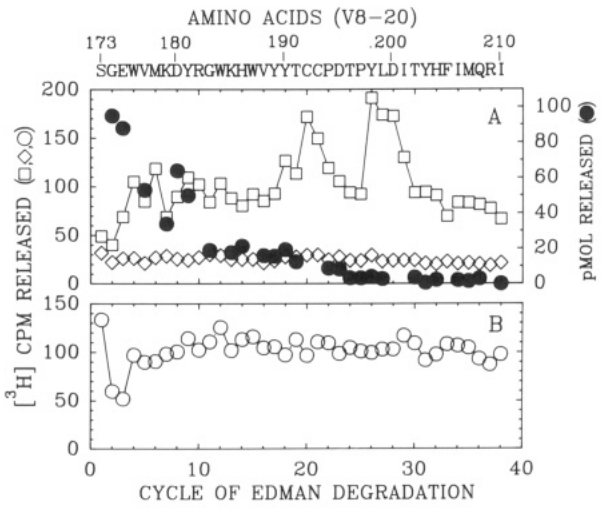

FIGURE 7: Radioactivity release upon sequential Edman degradation of [^{3}H]nicotine-labeled α-subunit and V8-20. (A) AChR-rich membranes (10 mg) were suspended in 6 mL of TPS (3 μM ACh sites) with 5 μM [^{3}H]nicotine/1 mM GSSG/20 μM proadifen in the absence or presence of 0.3 mM carbamylcholine. The membrane suspensions were irradiated for 4 min at 254 nm, collected by ultracentrifugation, and digested with endoglycosidase H, and the α-subunit was isolated and digested with V8 protease as described under Experimental Procedures. Approximately 40 μg of [^{3}H]-nicotine-labeled V8-20 labeled in the absence (□, ●, 45 000 cpm) or presence (◇, 2100 cpm) of carbamylcholine was sequenced for 38 cycles with $\approx$40% of each cycle analyzed for PTH-amino acids (●) and for ^{3}H (□, ◇). After 38 cycles, 13 500 cpm and 615 cpm remained on the filter. (B) About 40 μg of [^{3}H]nicotine-labeled α-subunit (○, 50 000 cpm) was sequenced for 38 cycles with $\approx$40% of each cycle analyzed for PTH-amino acids (data not shown) and for ^{3}H (○). After 38 cycles 19 500 cpm remained on the filter.

Table I: Yields of PTH-Amino Acids upon Sequence Analysis of V8-20[a]

		PTH-amino acids (pmol)	
cycle	S-173/S-162/S-1[b]	− carb	+ carb
1	Ser/Ser/Ser	NI/NI/NI	NI/NI/NI
2	Gly/Asp/Glu	238/75/55	312/44/28
3	Glu/Arg/His	220/88/18	335/48/11
4	Trp/Pro/Glu	21/118/NQ	55/98/NQ
5	Val/Asp/Thr	132/50/NI	275/62/NI
6	Met/Leu/Arg	X/X/X	370/90/22
7	Lys/Ser/Leu	85/NI/NQ	204/NI/NQ
8	Asp/Thr/Val	160/NI/25	222/NI/7
9	Tyr/Phe/Ala	125/25/15	218/45/6
10	Arg/Met/Asn	208/24/25	178/26/6

[a] The 20-kDa proteolytic fragment of [^{3}H]nicotine-labeled α-subunit generated by *S. aureus* V8 protease was isolated as described under Experimental Procedures. Figure 7A shows the corresponding release of ^{3}H for material labeled without (− carb) and with (+ carb) 0.4 mM carbamylcholine. A portion of each cycle ($\approx$40%) was used to detect PTH-amino acids, and the values shown are the calculated total release. [b] Starting residue and position in the α-subunit sequence for each sequence detected. NI indicates that the residue was present but not quantified because of instability of standards; NQ indicates that it was detected but not quantified because of lag from the same residue present in preceding cycle; X indicates failure of proper transfer of material to the HPLC.

release in those cycles was specific since no release was detected when nonspecifically labeled V8-20 (40 μg, 2600 cpm) was sequenced.

For V8-20, the primary sequence detected began at Ser-173 and that peptide was sequenced at 86% repetitive yield. In addition, peptides beginning at Ser-162 and Ser-1 were also detected at a lower level (Table I). The specific release of tritium in cycles 18, 20, and 26 could not originate from the amino-terminal fragment since no release was seen for intact

Table II: Yields of PTH-Amino Acids and ^{14}C upon Sequence Analysis of the Peak ^{14}C-Containing Fraction[a]

	PTH-amino acids (pmol)		
cycle	Thr-191[b]	Asn-94[b]	^{14}C released (cpm)
1	Thr (274)	Asn (302)	52
2	CMC (236)	Asn (316)	855
3	CMC (236)	Ala (326)	800
4	Pro (265)	Asp (278)	115
5	Asp (NQ)	Gly (167)	68
6	Thr (120)	Asp (NQ)	65
7	Pro (119)	Phe (66)	52
8	Tyr (90)	Ala (ND)	48
9	Leu (ND)	Ile (ND)	68
10	Asp (ND)	Val (ND)	50

[a] α-subunit (1 nmol) labeled by [^{14}C]iodoacetamide at Cys-192 and Cys-193 was digested with chymotrypsin, and the digest was fractionated by reversed phase HPLC as described under Experimental Procedures. ^{14}C was recovered in a single sharp peak at 17% acetonitrile (fraction 30), and 90% of that fraction was subjected to sequential Edman degradation. Each cycle was analyzed for PTH-amino acids (≈40%) and ^{14}C (counts per minute) released (≈40%), and values presented are the calculated total release. [b] Starting residue and position in the α-subunit sequence for each sequence detected. ND indicates that the residue was not detected; NQ indicates that it was detected but not quantified because of lag from the same residue present in the preceding cycle; CMC represents carboxamidomethylcysteine.

α-subunit. Similarly, the tritium released did not originate from the fragment beginning at Ser-162 since release was not detected in cycles 7, 9, and 15 as would be expected from the overlapping peptide beginning at Ser-173 that was present at a substantially higher level. Thus, the tritium was released from residues in the major peptide. These residues correspond to Tyr-190, Cys-192, and Tyr-198 of the AChR α-subunit.

Although the pattern of tritium release was complex and it is difficult to quantify lag and preview in long sequence runs, several considerations indicated that Tyr-198 contained the bulk of the photoincorporated [^3H]nicotine: (i) V8-20 was sequenced with a repetitive yield of 86%, so if the incorporation of tritium into Tyr-190 and Cys-192 was at the same level as the incorporation of tritium into Tyr-198 there would have been 10- and 4-fold greater releases of tritium in cycles 18 and 20 than the observed releases of 34 and 58 cpm, respectively. (ii) The ratio of specific release of tritium in cycle 26 (100 cpm) to the mass of PTH-Tyr (4 pmol) defined a specific incorporation of [^3H]nicotine at that residue (25 cpm/pmol) close to the specific incorporation of [^3H]nicotine into V8-20 (1200 cpm/μg or 24 cpm/pmol). In contrast, the specific incorporation into Tyr-190 and Cys-192 was closer to 2 and 4 cpm/pmol, respectively. However, less than 1% of α-subunits were labeled with [^3H]nicotine, and it remained possible that the observed tritium release did not originate from V8-20 but from a contaminating peptide not detectable by sequence analysis. To address that concern and to confirm that Tyr-198 was the principal site of incorporation, the sites of [^3H]nicotine labeling were analyzed by use of other proteases and a radiochemical sequencing strategy designed specifically to identify Tyr-198 as the site of photolabeling.

Chymotrypsin Digestion of the AChR α-Subunit. To further characterize the sites of incorporation of [^3H]nicotine in the α-subunit, we wanted to identify a protease that would generate unique, identifiable fragments in the region α-190–200. For a screening procedure, [^{14}C]carboxamidomethyl-α-subunit selectively alkylated at Cys-192 and Cys-193 (Kao & Karlin, 1986) was utilized, and digests were analyzed by reversed phase HPLC with an acetonitrile gradient. While digestion with trypsin (20% w/w) generated only hydrophobic radiolabeled material recovered in poor yield, digestion with chymotrypsin (20% w/w) allowed ^{14}C recovery in good yield

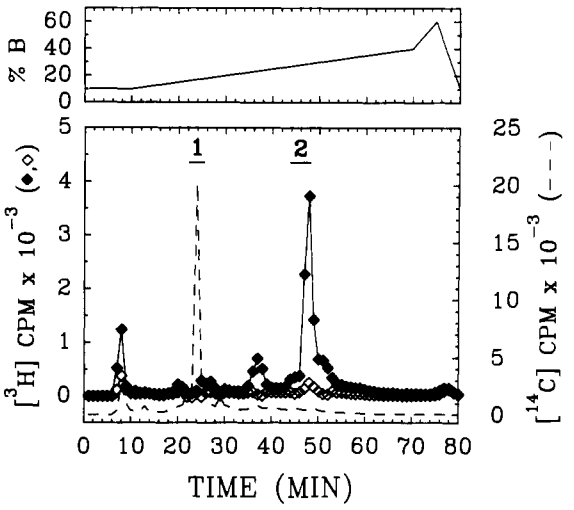

FIGURE 8: Reversed-phase HPLC separation of [^{14}C]iodoacetamide- and [^3H]nicotine-labeled α-subunit digested with chymotrypsin. α-Subunit was isolated from *Torpedo* membranes that had been photolabeled with [^3H]nicotine and then reduced and alkylated with [^{14}C]iodoacetamide on Cys-192 and Cys-193 (see Experimental Procedures). After being labeled in the absence of carbamylcholine, α-subunit contained 700 cpm of ^3H/μg (▲) and 1715 cpm of ^{14}C/μg (- - -), and in the presence of carbamylcholine, α-subunit contained 116 cpm of ^3H/μg (△) and 1590 cpm of ^{14}C/μg. α-Subunit (40 μg) was digested with 8.0 μg of chymotrypsin in 0.1 M NH_4HCO_3, pH 8.1/0.5% Lubrol-PX overnight at room temperature, and the digest was fractionated on a Vydac C-18 column with 0.1% TFA as solvent A and 0.09% TFA in acetonitrile as solvent B with a linear gradient of 10%–40% solvent B in 60 min. The eluted peptides were monitored by absorbance at 214 nm (data not shown) and scintillation counting of 50 μL-aliquots of 0.5-mL fractions for both ^3H (◆, ◇) and ^{14}C (- - -). ^3H and ^{14}C counts per minute were corrected for fraction volume, background, and emission energy overlap of ^{14}C into the ^3H energy range. For α-subunit labeled in the absence of carbamylcholine, 26 000 cpm of ^3H and 64 000 cpm of ^{14}C were loaded on the column, and 79 and 85% of loaded counts were recovered from the columns.

(83%), and a single sharp peak of ^{14}C was observed at 17% acetonitrile that contained >65% of recovered ^{14}C (data not shown). By sequence analysis (Table II), that fraction contained two peptides, α-191–198 and α-94–100, with release of ^{14}C in cycles 2 and 3 consistent with alkylation of both Cys-192 and Cys-193.

[^3H]Nicotine was photoincorporated into AChR, which was then alkylated selectively with [^{14}C]iodoacetamide at Cys-192 and Cys-193 of the α-subunit (see Experimental Procedures). When a chymotryptic digest of double-labeled α-subunit (0.8 nmol, 64 000 cpm ^{14}C, 26 000 cpm ^3H) was fractionated by reversed phase HPLC (Figure 8), ^{14}C eluted in a single peak (24 min, 17% acetonitrile), but that peak was well resolved from the principal peak of tritium (48 min, 29% acetonitrile). Minor peaks of ^3H (<20% of principal peak) eluted at 23% acetonitrile and with material not retained on the column in 10% acetonitrile. Fractions containing ^{14}C and ^3H were collected and characterized by protein microsequencing. The ^{14}C peak (fraction 24) contained α-191–198, and ^{14}C was released in cycles 2 and 3 of Edman degradation (data not shown). The level of ^3H in that fraction, which was 1.0% that of ^{14}C, was too low to quantify ^3H release during the sequence analysis. The principal peak of ^3H (fractions 46–48) contained many peptides on the basis of the presence of multiple PTH-amino acids in each cycle of Edman degradation, and conclusive assignment of the peptides present was difficult. However, release of ^3H (data not shown) was observed in the eighth cycle of Edman degradation, which would correspond to Tyr-198 if ^3H was contained on a peptide beginning at Thr-191.

To determine whether a peptide beginning at Thr-191 did account for the release of ^3H in cycle 8, we took advantage of the fact that there are two prolines on the amino-terminal side of Tyr-198 in the predicted peptide i.e., prolines at α-194 and α-197. *o*-Phthalaldehyde (OPA) reacts with primary amines but not with secondary amines, and it can be used at any cycle of Edman degradation to block the amino termini of all peptides except those with amino-terminal proline (Brauer et al., 1984). [^3H]Nicotine-labeled α-subunit was isolated from AChR that had been photolabeled in the absence or presence of carbamylcholine and then alkylated at Cys-192 and Cys-193 with nonradioactive iodoacetamide.[3] When a chymotryptic digest of [^3H]nicotine-labeled α-subunit (2 nmol, 127 000 cpm total label, 9000 cpm nonspecific label) was fractionated by reversed phase HPLC, three peaks of specific label were recovered (Figure 9). Forty-five percent of the specific ^3H was recovered in a principal peak (fractions 48–51, 25% acetonitrile) and shoulder (fractions 52–57), 18% of the ^3H was recovered at 22% acetonitrile (fractions 36–38), and 7% was recovered at 8% acetonitrile (fraction 18).

On the basis of microsequence analysis, the secondary peak (fractions 37–38) contained multiple peptides with no clear sequence assignments possible. When a sample containing 3900 cpm was sequenced, there was release of 580, 1530, and 640 cpm in the first three cycles of Edman degradation, with only 140 cpm retained on the filter after 13 cycles. For the tertiary peak (fraction 18, 6000 cpm), no clear sequence assignments were possible and no release of ^3H above background was detected during 22 cycles of Edman degradation, with 7% of the ^3H remaining on the filter.

Fractions 50 and 51 of the principal ^3H peak were combined and divided into four equal aliquots for sequence analysis with and without the use of OPA. When two aliquots were sequenced up to 24 cycles without exposure to OPA, there was specific release of ^3H in cycle 8 only (Figure 10). For a sample reacted with OPA immediately after cycles 3 and 6, the release of ^3H in cycle 8 remained, while for a sample reacted with OPA immediately after the fifth cycle of Edman degradation, the subsequent release of ^3H was prevented. In addition, and as expected, exposure to OPA at any stage prevented subsequent sequencing of the peptide beginning at Asp-152, which was the only mass detectable in these fractions (Table III). Sequence analysis of the other fractions from the primary peak (fractions 48 and 49) revealed release of ^3H only in the eighth cycle of Edman degradation (data not shown). Because Pro-194 and Pro-197 are the only two prolines in the α-subunit separated by two residues, the results of the radiochemical sequence analyses establish that the release of ^3H in cycle 8 originated from Tyr-198.

Discussion

The studies presented here characterize the reversible binding of [^3H]nicotine by *Torpedo* membranes and establish conditions for its covalent incorporation into the ACh binding sites by use of UV irradiation. Although nicotine at high concentrations inhibits the binding of the noncompetitive antagonist [^3H]perhydrohistrionicotoxin (K_I = 650 μM; Eldefrawi et al., 1982), at concentrations up to 15 μM, [^3H]nicotine binds with high selectivity to the ACh site. [^3H]Nicotine was bound to the same number of sites in the presence and absence of the noncompetitive antagonist proadifen, but with three-fold higher affinity in the presence of proadifen than in its absence. That increase in affinity is the same as that proadifen produces on the binding of [^3H]ACh and reflects the fact that both proadifen and agonists bind preferentially to the same desensitized state of the AChR (Boyd & Cohen, 1984). On the basis of the inhibition of [^3H]nicotine binding by *d*-tubocurarine, nicotine binds at equilibrium with similar affinity to the two ACh sites. Even when only $\approx$10% of sites were occupied by [^3H]nicotine, the concentration dependence of the inhibition of binding by *d*-tubocurarine (Figure 1B) is as expected for nicotine distributed approximately equally between the sites binding *d*-tubocurarine with high and low affinity.

UV irradiation at 254 nm of membrane suspensions equilibrated with [^3H]nicotine resulted in covalent incorporation of [^3H]nicotine primarily into AChR α- and γ-subunits. This labeling was inhibited by agonists and competitive antagonists but not by noncompetitive antagonists. The lack of effect of oxidized glutathione on the specific photolabeling is consistent with the direct photoincorporation of bound [^3H]-nicotine prior to its dissociation from and diffusion out of the binding site. Even under conditions where the agonist sites were >90% occupied by nicotine, 90% of the labeling of α-subunit was inhibited by carbamylcholine, while for γ-subunit 70% of the labeling was specific. Both the dependence of photolabeling upon [^3H]nicotine concentration and its inhibition by carbamylcholine and *d*-tubocurarine were consistent with photolabeling of AChR α-subunits by [^3H]nicotine bound to either of the agonist sites while photolabeling of the γ-subunit was by [^3H]nicotine bound only to the site with high affinity for *d*-tubocurarine. The photolabeling of AChR γ-subunit by [^3H]nicotine is consistent with results obtained with [^3H]-*d*-tubocurarine, which is photoincorporated into α- and γ-subunits when bound to its high-affinity site (Pedersen & Cohen, 1990). Unlike [^3H]-*d*-tubocurarine, there was no evidence that [^3H]nicotine was photoincorporated into the AChR δ-subunit when bound to the agonist site binding *d*-tubocurarine with low affinity despite the fact that similar irradiation conditions were used for the two ligands. The lack of δ-subunit labeling suggests that bound [^3H]nicotine, which is smaller than *d*-tubocurarine, is not in proximity to the same residues in the δ-subunit as *d*-tubocurarine.

Upon irradiation at 254 nm the efficiency of photoincorporation was low. Irradiation for 10 min resulted in specific labeling of $\approx$0.4% of α-subunits and 0.2% of γ-subunits, and the presence of proadifen did not alter the efficiency of photoincorporation into either subunit or enhance labeling of other subunits. While longer irradiation times did produce greater photolabeling, there was also substantial photo-cross-linking of membrane polypeptides. In an attempt to determine the action spectrum for photolabeling, irradiation at 254 nm was compared with that at 280 and 300 nm. Little photoincorporation was detected at 300 nm, and at 280 nm there was no significant increase in the specific incorporation relative to photo-cross-linking.

Because photoincorporation was detected under conditions where both nicotine and amino acid side chains are excited, it is not possible to determine which component generates the initial reactive species. The strained vicinal disulfide Cys-192/Cys-193 might have been expected to be the site of photoreactivity since cleavage of disulfides has long been recognized as a consequence of protein irradiation at 254 nm, and the molar extinction coefficient of cystine at 254 nm is the same as tyrosine (McClaren & Shugar, 1964). Even before the direct analysis of the sites of photolabeling, this

[3] Receptors were alkylated at α-Cys-192 and Cys-193 with nonradioactive iodoacetamide because in the analysis of [^3H]nicotine distribution and recovery from the chymotryptic digest of ^3H- and ^{14}C-labeled α-subunit (Figure 8), it was difficult to quantify ^3H eluting in fractions that contained larger amounts of ^{14}C.

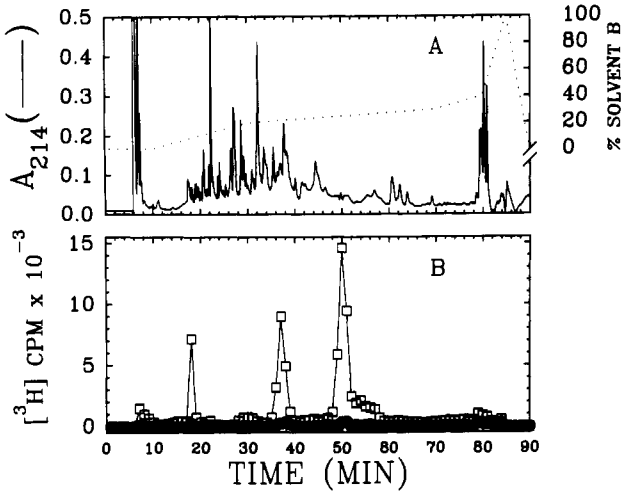

FIGURE 9: Reversed-phase HPLC separation of a chymotryptic digest of [^{3}H]nicotine-labeled α-subunit. Purified α-subunit (100 μg) labeled with [^{3}H]nicotine in the absence (□, 127 000 cpm) or presence (●, 9000 cpm) of carbamylcholine and alkylated with nonradioactive iodoacetamide on Cys-192 and Cys-193 (see Experimental Procedures) was digested with 20 μg of chymotrypsin in 0.1 M NH_4HCO_3, pH 8.1/0.5% Lubrol-PX overnight at room temperature. The digest was fractionated on a Vydac C-18 column with the indicated gradient (solvent A, 0.1% aqueous TFA; solvent B, 0.09% TFA in acetonitrile). The peptides eluted were monitored by absorbance at 214 nm (A) and by scintillation counting of 25-μL aliquots of 0.5-mL fractions. The total counts per minute per fraction is plotted (B). For α-subunits labeled in the absence or presence of carbamylcholine, 79 and 83% of the loaded ^{3}H was recovered from the columns.

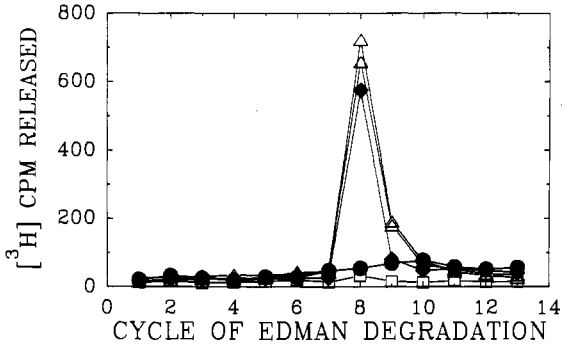

FIGURE 10: Radioactivity released upon sequence analysis of the principal [^{3}H]nicotine-labeled chymotryptic peptide. Material eluting in fractions 50–51 (Figure 9) was pooled and divided into four aliquots (220 μL) that were stored at −80 °C until sequence analysis. Aliquots (3600 cpm) from α-subunit labeled in the absence of carbamylcholine (△, ◆, ●) were either sequenced normally (△, 2 samples) or treated with o-phthalaldehyde (OPA) after the third and sixth cycles (◆) or after the fifth cycle (●) of Edman degradation as described under Experimental Procedures. Counts per minute remaining on the filters were 560 (△, 13 cycles), 330 (△, 26 cycles), 710 (◆, 15 cycles), and 1310 (●, 13 cycles). For α-subunit labeled nonspecifically (□), an aliquot (200 cpm) was sequenced normally with 15 cpm recovered on the filter after 13 cycles.

appeared unlikely because [^{3}H]nicotine incorporation into the γ-subunit was nearly as efficient as that into the α-subunit. Direct analysis of the pattern of photolabeling of the α-subunit established that labeling of Cys-192 and Cys-193 accounted for only a small fraction of the specific photolabeling.

Within the α-subunit, 93% of the specific photoincorporation was restricted to a 20-kDa proteolytic fragment (V8-20) beginning at Ser-173. On the basis of microsequence analysis and adjustment for repetitive yield, ≈80% of this specific labeling was associated with Tyr-198, ≈13% with Cys-192, and ≈7% with Tyr-190. Because it is difficult to quantify yields from long sequencing runs, this conclusion was confirmed by analysis of [^{3}H]nicotine-labeled peptides generated by chymotryptic digestion of labeled α-subunit. Following fractionation by reversed phase HPLC, the principal ^{3}H-labeled peptide, containing ≈50% (Figures 8 and 9) of the recovered ^{3}H, was shown to begin at Thr-191 and to be labeled only at Tyr-198. The labeled peptide was not detected by mass but was identified unambiguously by taking advantage of the fact that it is the only sequence in the α-subunit containing prolines two residues apart (Pro-194 and Pro-197). When o-phthalaldehyde was used to block free amino termini after the third and sixth cycles of Edman degradation, full release of radioactivity was still detected at the eighth cycle. Two reasons for separation of this radiolabeled peptide from the chymotryptic fragment α-191-198 are possible: (1) The incorporated [^{3}H]nicotine alters the mobility of the fragment or (2) labeling of Tyr-198 prevents chymotryptic cleavage at that site.

While the sequence analysis of the principal ^{3}H peak isolated by reversed-phase HPLC from the chymotryptic digest identified unambiguously Tyr-198 as the primary site of photolabeling, characterization of the secondary ^{3}H peak was less conclusive. Fractions 36–38 (Figure 9), containing half as many counts as the principal ^{3}H peak, eluted at 22% acetonitrile, closer to the position observed for ^{14}C α-191–198 (17% acetonitrile, Figure 8). Upon microsequence analysis, counts were released primarily in the second but also in the first and third cycles of Edman degradation. Release in cycles 2 and 3 would be consistent with the presence of α-191–198 and labeling of Cys-192 and Cys-193. The release of ^{3}H observed in the first cycle might reflect labeling of Thr-191 or the presence of additional radiolabeled peptides in that fraction. Alternative proteolytic digests will be required to confirm the relative labeling of Tyr-190 and Cys-192/Cys-193 estimated from the sequence analysis of V8-20.

The results obtained with [^{3}H]nicotine establish that an agonist affinity label, like previous antagonist affinity labels, reacts with amino acids contained between α-191 and α-198. It is striking, however, that the agonist labels Tyr-198 preferentially while [^{3}H]lophotoxin analogue 1 reacts solely with Tyr-190 (Abramson et al., 1989) and [^{3}H]-*p*-(dimethylamino)benzenediazonium fluoroborate (DDF) is photoincorporated into Tyr-190 and Cys-192/193 with labeling of Tyr-198 minor, if at all (Dennis et al., 1988). Lophotoxin analogue 1 has intrinsic, uncharacterized chemical reactivity, and AChR alkylation does not depend upon photoactivation. [^{3}H]DDF is believed to form a reactive aryl cation following excitation by energy transfer from protein and loss of molecular nitrogen. Thus, it is possible that preferential alkylation of Tyr-198 does not reflect an intrinsic difference between agonists and antagonists but a preferential reactivity of that residue under conditions used for photoactivation. This interpretation is unlikely because [^{3}H]-*d*-tubocurarine, which specifically photolabels α-subunit upon irradiation at 254 nm (Pedersen & Cohen, 1990), has been shown to label Tyr-190 and Cys-192 preferentially (D. Chiara and J.B.C., unpublished experiments).

Thus, the preferential alkylation by [^{3}H]nicotine of Tyr-198 must result from the intrinsic reactivity of [^{3}H]nicotine and/or its orientation within the ACh binding site. Unfortunately, it is not possible to predict whether the aromatic (pyridine) or aliphatic (pyrrolidine) ring is the site of photoaddition. Irradiation at 254 nm of pyridine in a nonaqueous environment results in radical mediated photoaddition reactions (Caplain et al., 1971), and for nicotine, at least in the presence of photosensitizers, 254-nm excitation results in endocyclic

Table III: Yields of PTH-Amino Acids upon Sequence Analysis of the Principal ^3H Containing Fractions: Effects of OPA[a]

		PTH-amino acids (pmol)		
cycle	Asp-152[b]	no OPA	OPA(3,6)[c]	OPA(5)[c]
1	Asp	60/79	90	56
2	Gly	37/49	99	39
3	Thr	NI/NI	NI	NI
4	Lys	42/40	ND	46
5	Val	39/27	ND	31
6	Ser	NI/NI	ND	ND
7	Ile	41/25	ND	ND
8	Ser	NI/NI	ND	ND
9	Pro	19/14	ND	ND
10	Glu	10/15	ND	ND

[a] Fractions 50 and 51 from the chymotryptic digest of [^3H]nicotine-labeled α-subunit (Figure 9) were pooled, and aliquots were subjected to sequence analysis as described in Figure 10 where the corresponding ^3H releases are plotted. A portion of each cycle (≈40%) was used to detect PTH-amino acids, and the values shown are the calculated total release. [b] Starting residue and position in the α-subunit. [c] Cycles of Edman degradation after which the automated sequencer was paused in order to react the peptides with OPA as described under Experimental Procedures. ND indicates that the residue was not detected; NI indicates that it was not integrated.

photoaddition to the pyrrolidine ring (Hubert-Brierre et al., 1975). While our results establish the proximity of Tyr-198 to the agonist sites, they do not directly establish the contribution made by interactions with Tyr-198 to the free energy of nicotine binding. Tyr-198, like Tyr-190, Cys-192, Cys-193, and Asp-200, is absolutely conserved across all nicotinic AChR α-subunit sequences (Couturier et al., 1990), and additional studies will be required to determine whether certain of these residues are more important for the binding of agonists than antagonists.

ACKNOWLEDGMENTS

We thank Dr. Wu-Schyong Liu for developing and testing the *o*-phthalaldehyde reaction protocol used in this work and for many valuable comments and suggestions for sequence analysis. We also thank Dr. Steen Pedersen, Ben White, and David Chiara for their helpful suggestions.

Registry No. ACh, 51-84-3; Tyr, 60-18-4; nicotine, 54-11-5; *o*-phthalaldehyde, 643-79-8.

REFERENCES

Abramson, S. N., Li, Y., Culver, P., & Taylor, P. (1989) *J. Biol. Chem. 264*, 12666–12672.

Betz, H. (1990) *Neuron 5*, 383–392.

Boyd, N. D., & Cohen, J. B. (1980) *Biochemistry 19*, 5344–5353.

Boyd, N. D., & Cohen, J. B. (1984) *Biochemistry 23*, 4023–4033.

Brauer, A. W., Oman, C. L., & Margolies, M. N. (1984) *Anal. Biochem. 137*, 134–142.

Caplain, S., Castellano, A., Catteau, J.-P., & Lablache-Combier, A. (1971) *Tetrahedron 27*, 3541–3553.

Carr, C., McCourt, D., & Cohen, J. B. (1987) *Biochemistry 26*, 7090–7102.

Claudio, T. (1989) in *Frontiers in Molecular Biology: Molecular Neurobiology* (Glover, D. M., & Hames, B. D., Eds.) pp 63–142, IRL Press, Oxford.

Cleveland, D. W., Fischer, S. G., Kirschner, M. W., & Laemmli, U. K. (1977) *J. Biol. Chem. 252*, 1102–1106.

Cohen, J. B., Medynski, D. C., & Strnad, N. P. (1985) in *Effects of Anesthesia* (Covino, G., Fozzard, H. A., Rehder, K., & Strichartz, G., Eds.) pp 53–63, American Physiological Society, Bethesda.

Couturier, S., Bertrand, D., Matter, J.-M., Hernandez, M.-C., Bertrand, S., Millar, N., Valera, S., Barkas, T., & Ballivet, M. (1990) *Neuron 5*, 847–856.

Damle, V. N., McLaughlin, M., & Karlin, A. (1978) *Biochem. Biophys. Res. Commun. 84*, 845–851.

Dennis, M., Giraudat, J., Kotzyba-Hibert, F., Goeldner, M., Hirth, C., Chang, J.-Y., Lazure, C., Chrêtien, M., & Changeux, J.-P. (1988) *Biochemistry 27*, 2346–2357.

Dreyer, E. B., Hasan, F., Cohen, S. G., & Cohen, J. B. (1986) *J. Biol. Chem. 261*, 13727–13734.

Eldefrawi, A. T., Miller, E. R., & Eldefrawi, M. E. (1982) *Biochem. Pharmacol. 31*, 1819–1822.

Forman, S. A., Firestone, L. L., & Miller, K. W. (1987) *Biochemistry 26*, 2807–2814.

Galzi, J.-L., Revah, F., Black, D., Goeldner, M., Hirth, C., & Changeux, J.-P. (1990) *J. Biol. Chem. 265*, 10430–10437.

Giraudat, J., Dennis, M., Heidmann, T., Haumont, P.-Y., Lederer, F., & Changeux, J.-P. (1987) *Biochemistry 26*, 2410–2418.

Heidmann, T., Oswald, R. E., & Changeux, J.-P. (1983) *Biochemistry 22*, 3112–3127.

Hubert-Brierre, Y., Herlem, D., & Khuong-Huu, F. (1975) *Tetrahedron 31*, 3049–3054.

Hucho, F., Oberthür, W., & Lottspeich, F. (1986) *FEBS Lett. 205*, 137–142.

Kao, P. N., & Karlin, A. (1986) *J. Biol. Chem. 261*, 8085–8088.

Kao, P. N., Dwork, A. J., Kaldany, R. J., Silver, M. L., Wideman, J., Stein, S., & Karlin, A. (1984) *J. Biol. Chem. 259*, 11662–11665.

Kellaris, K. V., & Ware, D. K. (1989) *Biochemistry 28*, 3469–3482.

Krodel, E. K., Beckman, R. A., & Cohen, J. B. (1979) *Mol. Pharmacol. 15*, 294–312.

Kubalek, E., Ralston, S., Lindstrom, J., & Unwin, N. (1987) *J. Cell Biol. 105*, 9–18.

McLaren, A. D., & Shugar, D. (1964) *Photochemistry of Proteins and Nucleic Acids*, Pergamon Press Inc., New York.

Mitra, A. K., McCarthy, M. P., & Stroud, R. M. (1989) *J. Cell Biol. 109*, 755–774.

Neubig, R. R., & Cohen, J. B. (1979) *Biochemistry 18*, 5464–5475.

Neubig, R. R., Boyd, N. D., & Cohen, J. B. (1982) *Biochemistry 21*, 3460–3467.

Noda, M., Takahashi, H., Tanabe, T., Toyosato, M., Kikyotani, S., Furutani, Y., Hirose, T., Takashima, H., Inayama, S., Miyata, T., & Numa, S. (1983) *Nature (London) 302*, 528–532.

Pedersen, S. E., & Cohen, J. B. (1990) *Proc. Natl. Acad. Sci. U.S.A. 87*, 2785–2789.

Pedersen, S. E., Dreyer, E. B., & Cohen, J. B. (1986) *J. Biol. Chem. 261*, 13735–13743.

Popot, J.-L., & Changeux, J.-P. (1984) *Physiol. Rev. 64*, 1162–1239.

Raftery, M. A., Hunkapiller, M. W., Strader, C. D., & Hood, L. E. (1980) *Science 208*, 1454–1457.

Revah, F., Galzi, J.-L., Giraudat, J., Haumont, P.-Y., Lederer, F., & Changeux, J.-P. (1990) *Proc. Natl. Acad. Sci. U.S.A. 87*, 4675–4679.
Schaffner, W., & Weissmann, C. (1973) *Anal. Biochem. 56*, 502–514.
Singh, S. P., Stenberg, V. I., & Parmar, S. S. (1980) *Chem. Rev. 80*, 269–282.
Sobel, A., Weber, M., & Changeux, J.-P. (1977) *Eur. J. Biochem. 80*, 215–224.
Stroud, R. M., McCarthy, M. P., & Shuster, M. (1990) *Biochemistry 29*, 11009–11023.
Toyoshima, C., & Unwin, N., (1988) *Nature (London) 336*, 247–250.
Weiland, G., & Taylor, P. (1979) *Mol. Pharmacol. 15*, 197–212.
White, B. H., & Cohen, J. B. (1988) *Biochemistry 27*, 8741–8751.
Whitten, D. G. (1976) in *Photochemistry of Heterocyclic Compounds* (Buchardt, O., Ed.) pp 524–573, John Wiley & Sons, New York.

Transbilayer Distribution of Bromine in Fluid Bilayers Containing a Specifically Brominated Analogue of Dioleoylphosphatidylcholine†

Michael C. Wiener and Stephen H. White*
Department of Physiology and Biophysics, University of California, Irvine, California 92717
Received January 22, 1991; Revised Manuscript Received April 17, 1991

ABSTRACT: We describe in this paper the transbilayer distribution of the bromines of the specifically halogenated phospholipid 1-oleoyl-2-(9,10-dibromostearoyl)-*sn*-glycero-3-phosphocholine (OBPC). The distribution was determined by X-ray diffraction of oriented multilayers of mixtures of OBPC and 1,2-dioleoyl-*sn*-glycero-3-phosphocholine (DOPC) at 66% relative humidity by the general approach of Franks et al. (1978) [*Nature 276*, 530–532]. The bromine distribution of OBPC in the fluid L_α phase is described accurately by a pair of Gaussian functions located 7.97 ± 0.27 Å from the center of the bilayer with $1/e$ half-widths of 4.96 ± 0.62 Å. We find that OBPC bilayers are accurately described as DOPC bilayers with an additional bromine distribution centered at the position of the double bond of DOPC and conclude that OBPC is an excellent structural isomorph for DOPC under the conditions of these experiments. The distribution obtained is the complete and fully resolved transbilayer image of the halogen label because the broad distribution of the bromines is due entirely to thermal disorder and not to experimental limitations [Wiener, M. C., & White, S. H. (1991a) *Biophys. J. 59*, 162–173]. The observed width of the bromine distribution indicates that virtually all of the hydrocarbon interior is accessible to the bromines. The distance between the bromine/double-bond position and the headgroup phosphate position was determined from one-dimensional Patterson maps and found to be ≈12 Å. The application of accurately determined bromine distributions to the quantitative interpretation of fluorescence quenching experiments is discussed. A method for the self-consistent global analysis of diffraction data from mixtures that permits the use of data sets with different instrumental scale factors is developed in an Appendix.

Fluorescence spectroscopy is an important experimental method for investigating biomolecules in membrane environments [see Lakowicz (1983)]. Of particular interest are fluorescence energy transfer (Kleinfeld, 1985; Kleinfeld & Lukacovic, 1985) and fluorescence quenching (Markello et al., 1985; Blatt & Sawyer, 1985; Everett et al., 1986; Chattopadhyay & London, 1987) methods used to determine the positions of fluorophores in membranes. The fluorophores are typically endogenous tryptophans of membrane proteins, labels attached to proteins, or labeled lipids. The elegant and promising "parallax method" of Chattopadhyay and London (1987) can be used to determine the depth of a fluorophore in a membrane by measuring the degree of quenching by two labels at different positions within the bilayer. However, this method, like all others, requires prior estimates of the average positions of the fluorescence quenchers (or acceptors) in order to obtain the accurate position of the donor fluorophore. In addition, the transbilayer distributions of acceptors or quenchers across the bilayer may influence the interpretation of fluorescence experiments or the theoretical models on which their interpretation is based.

Brominated lipids have been used as fluorescence quenchers (Leto et al., 1980; East & Lee, 1982; Holloway et al., 1982; Markello et al., 1985; Everett et al., 1986) and several recent papers attest to continued interest in using specifically brominated phospholipids for examining membrane structure (Silvius, 1990; Yeager & Feigenson, 1990; De Kroon et al., 1990). X-ray diffraction is an excellent method for determining the positions and distributions of heavy atoms and other labels within bilayers (Lesslauer et al., 1971, 1972; McIntosh et al., 1976; Franks et al., 1978; Lytz et al., 1984; McIntosh & Holloway, 1987; Trumbore et al., 1988; Mason et al., 1989; Katsaras & Stinson, 1990) and thus can provide crucial information for the analysis of quenching data. We describe in this paper the fully resolved transbilayer distribution of bromines of the specifically halogenated phospholipid 1-oleoyl-2-(9,10-dibromostearoyl)-*sn*-glycero-3-phosphocholine (OBPC,[1] shown in Figure 1). We have determined the

†This work was supported by grants from the National Science Foundation (DMB-880743) and the National Institute of General Medical Sciences (GM-37291).
* Author to whom correspondence should be addressed.

[1] Abbreviations: OBPC, 1-oleoyl-2-(9,10-dibromostearoyl)-*sn*-glycero-3-phosphocholine; DOPC, 1,2-dioleoyl-*sn*-glycero-3-phosphocholine; 18:1 lysoPC, 1-oleoyl-*sn*-glycero-3-phosphocholine; TLC, thin-layer chromatography; HPLC, high-performance liquid chromatography; EtOH, ethanol; MeOH, methanol.

0006-2960/91/0430-6997$02.50/0